# Multi-frequency Imaging of Multiple Targets in Rician Fading Media

## *Stability and Resolution*

Pengchong(Mike) Yan

Collaborated with Prof. Albert Fannjiang

Math Department

University of California at Davis

# Paper

- A. Fannjiang and P. Yan, *Multi-frequency imaging of multiple targets in Rician fading channels: stability and resolution*. *Inverse Problems* 23 (2007), 1801-1819.

# Outline

- Mathematical Models and Simulations
- Active Array Model and its Stability
- Passive Array Model and its Stability
- Conclusion

# Mathematical Models

- Acoustic wave equation:

$$\Phi_{tt} - c^2(\mathbf{x})\Delta\Phi = c^2(\mathbf{x}) f(\mathbf{x}, t)\delta(\mathbf{x} - \mathbf{x}_s)$$

- In the frequency domain: Helmholtz equation

$$\begin{aligned} \Delta\hat{\Phi} + \frac{\omega^2}{c^2}\hat{\Phi} &= -\hat{f}(\mathbf{x}, \omega)\delta(\mathbf{x} - \mathbf{x}_s) \\ \Delta\hat{\Phi} + \frac{\omega^2}{c_0^2}(1 + n^2(\mathbf{x}))\hat{\Phi} &= -\hat{f}(\mathbf{x}, \omega)\delta(\mathbf{x} - \mathbf{x}_s). \end{aligned}$$

- Assume media noise $n^2(\mathbf{x}) = \sum_{j=1}^{J} \tau_j \delta(\mathbf{x} - \mathbf{x}_j)$. Then the Lippmann-Schwinger equation becomes in this case

$$\hat{\Phi}(\mathbf{x}; \omega_l) = \hat{\Phi}^{(\mathrm{in})}(\mathbf{x}; \omega_l) + \sum_{j=1}^{J} \tau_j(\omega_l) G_0(\mathbf{x}, \mathbf{x}_j; \omega_l)\hat{\Phi}(\mathbf{x}_j; \omega_l)$$

# Numerical Setup

- Antennas

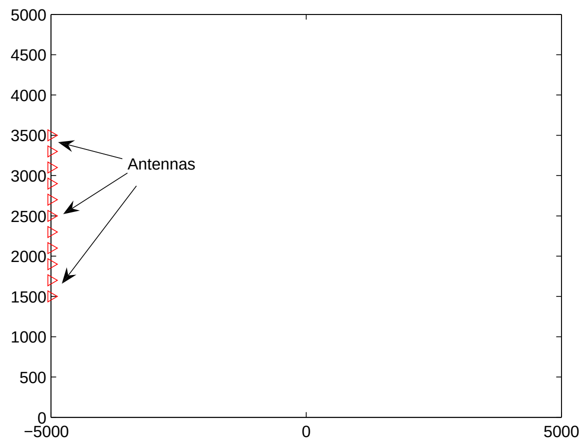

# Numerical Setup

- Antennas
- Point-clutter

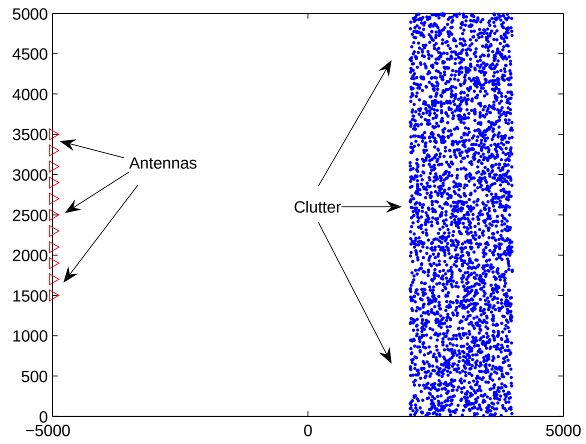

# Numerical Setup

- Antennas
- Point-clutter

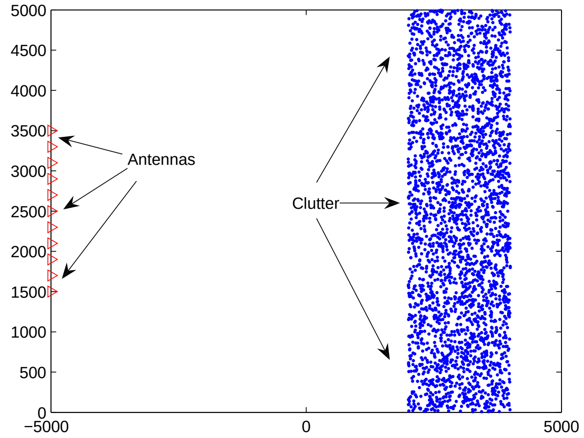


The Lippmann-Schwinger equation is valid for all $\mathbf{x}$ except at the actual scatterer locations $\mathbf{x} = \mathbf{x}_i$. So to determine $\hat{\Phi}(\mathbf{x}_j; \omega_l)$, we replace the Lippmann-Schwinger equation by the Foldy-Lax formula:

$$\hat{\Phi}(\mathbf{x}_i; \omega_l) = \hat{\Phi}^{(\mathrm{in})}(\mathbf{x}_i; \omega_l) + \sum_{j \neq i} \tau_j(\omega_l) G_0(\mathbf{x}_i, \mathbf{x}_j; \omega_l) \hat{\Phi}(\mathbf{x}_j; \omega_l).$$

# Classification

- In the active array model, we sent signals out to probe the media. The received signals at the transducers organize the response matrices.
  For example:
  - Far field imaging: Radar
  - Near field imaging: Magnetic resonance imaging (MRI)
- In the passive array model, the wave source is far away from the receivers.
  For examples:
  - earthquake seismic waves,
  - seismic waves excited by the pounding of the ocean waves and the wind,
  - stars in the sky.

# Outline

- Mathematical Models and Simulations
- Active Array Model and its Stability
- Passive Array Model and its Stability
- Conclusion

# Differential Responses

- In this approach, probing signals of various frequencies are sent out twice, before and after the intrusion of the targets.
- **Advantage:**
  The medium uncertainty is reduced by subtracting the clutter response (without targets) as we are only interested in the change (i.e. inclusion of targets) in the cluttered medium.
- **Media Assumption:**
  The media are assumed to be fixed in both cases. Then the differential responses (square matrices) is given by

$$R_{n,j} = \sum_{i=1}^{M} \tau(\mathbf{x}_i) H(\mathbf{x}_i, \mathbf{y}_n; \omega_l) H(\mathbf{x}_i, \mathbf{y}_j; \omega_l)$$

# Singular Value Decomposition

For easy illustration, we look at the homogeneous case first:

$$\vec{G}(\mathbf{x}_1, \omega) = \begin{pmatrix} G_0(\mathbf{x}_1, \mathbf{y}_1; \omega) \\ G_0(\mathbf{x}_1, \mathbf{y}_2; \omega) \\ \vdots \\ G_0(\mathbf{x}_1, \mathbf{y}_N; \omega) \end{pmatrix}$$

The response is

$$R(\omega) = \sum_{i=1}^{M} \tau_i(\omega) \vec{G}(\mathbf{x}_i, \omega) \vec{G}(\mathbf{x}_i, \omega)^T$$

If $N > M$, the dominant left singular vectors have the information of the targets' locations.

# MUltiple SIgnal Classification (MUSIC)

MUSIC algorithm can improve the resolution in imaging.

- Idea:
  - $\vec{G}(\mathbf{x}_i, \omega) \in \mathcal{N}(U_L^i)$, where $U_L^i$ denotes the insignificant left singular vectors.
  - Image the inverse of the projection $\vec{G}(\mathbf{x}, \omega)$ onto $\mathcal{R}(U_L^i)$.
- Advantages: Targets pop out (valued $\infty$).
- Disadvantages:
  - Unable to handle the case when $N < M$.
  - MUSIC algorithm works OK for small noise, but the resolution is not as good as the homogeneous case.
  - MUSIC fails with big noise.

# Imaging

The imaging function

$$\begin{aligned} u(\mathbf{x}) &= \sum_{\omega_l=1}^{B} \vec{P}^T(\mathbf{x};\omega_l)R(\omega_l)\vec{P}(\mathbf{x};\omega_l) \\ &= \sum_{l=1}^{B}\sum_{i=1}^{M}\sum_{j,n=1}^{N} \tau_i(\omega_l)P(\mathbf{x},\mathbf{y}_j;\omega_l)H_{ij}(\omega_l)H_{in}(\omega_l)P(\mathbf{y}_n,\mathbf{x};\omega_l). \end{aligned}$$

- $H_{ij}(\omega_l) = H(\mathbf{x}_i,\mathbf{y}_j;\omega_l)$ is the full Green's function of the medium at the frequency $\omega_l$ from antenna $\mathbf{y}_j$ to the scatterer $\mathbf{x}_i$
- $P$ is back-propagator filter (the mean-phase-matched filter), i.e.

$$P(\mathbf{x},\mathbf{y};\omega) = \frac{\bar{H}^*(\mathbf{x},\mathbf{y};\omega)}{|\bar{H}(\mathbf{x},\mathbf{y};\omega)|}$$

# Simplifications of the Model

We decompose the random full Green's function into the mean $\bar{H}$ and the fluctuation $h, \mathbb{E}h = 0$, as

$$H(\mathbf{x}, \mathbf{y}; \omega) = \bar{H}(\mathbf{x}, \mathbf{y}; \omega) + h(\mathbf{x}, \mathbf{y}; \omega).$$

- $h_{ij}, \forall i, j$, are circularly Gaussian random variables with zero mean;

  $$\mathbb{E}\Big\{h_{ij}(\omega_k)h^*_{mn}(\omega_l)\Big\} \approx \eta^2\delta_{im}\delta_{jn}\delta_{k,l}, \mathbb{E}\Big\{h_{ij}(\omega_k)h_{mn}(\omega_l)\Big\} \approx 0, \forall i, j, m, n, k, l$$

  where $\eta^2$ is the intensity of fluctuations.
- the separations of the frequencies $\omega_l, l = 1, 2, ..., B$ used for imaging are larger than the coherence bandwidth $\beta_c$ of the cluttered medium;
- the spacings of the antennas are wider than the coherence length $\ell_c$ of the cluttered medium.

# Stability Condition

- Let $\mu$ be the typical magnitude of the *mean* full Green's function and let $K$ be the Rician factor defined as

$$K = \frac{\mu^2}{\eta^2}.$$

- We define the stability condition as:

$$\mathfrak{R}(\mathbf{x}) \equiv \frac{|\mathbb{E}u(\mathbf{x})|^2}{\mathbb{E}\big(|u|^2(\mathbf{x})\big) - |\mathbb{E}\big(u(\mathbf{x})\big)|^2} \to \infty$$

- Results: The imaging function is stable when $KBN \gg M$.

# Sketch of the Proof

The imaging function

$$u(\mathbf{x}) = \sum_{l=1}^{B}\sum_{i=1}^{M}\sum_{j,n=1}^{N} \tau_i(\omega_l) P(\mathbf{x}, \mathbf{y}_j; \omega_l)\big(\bar{H}_{ij}(\omega_l) + h_{ij}(\omega_l)\big) \times \big(\bar{H}_{in}(\omega_l) + h_{in}(\omega_l)\big) P(\mathbf{y}_n, \mathbf{x}; \omega_l).$$

The expectation of $u$ is then given by

$$\mathbb{E}u(\mathbf{x}) = \sum_{l=1}^{B}\sum_{i=1}^{M}\sum_{j,n=1}^{N} \tau(\omega_l) P(\mathbf{x}, \mathbf{y}_j; \omega_l) \bar{H}_{ij} \bar{H}_{in}(\omega_l) P(\mathbf{y}_n, \mathbf{x}; \omega_l) = O(\mu^2 B N^2).$$

# Sketch of the Proof (Cont'd)

$$
\begin{aligned}
\mathbb{E}|u(\mathbf{x})|^2 \;&\approx\; \Big|\sum_{l=1}^{B}\sum_{i=1}^{M}\sum_{j,n=1}^{N} \tau(\omega_l) P(\mathbf{x},\mathbf{y}_j;\omega_l)\bar{H}_{ij}\bar{H}_{in}(\omega_l)P(\mathbf{y}_n,\mathbf{x};\omega_l)\Big|^2 \\
&+\; \mathbb{E}\Big|\sum_{l=1}^{B}\sum_{i=1}^{M}\sum_{j,n=1}^{N} \tau(\omega_l) P(\mathbf{x},\mathbf{y}_j;\omega_l)\big(\bar{H}_{ij}h_{in} + h_{ij}\bar{H}_{in}\big)P(\mathbf{y}_n,\mathbf{x};\omega_l)\Big|^2 \\
&+\; \mathbb{E}\Big|\sum_{l=1}^{B}\sum_{i=1}^{M}\sum_{j,n=1}^{N} \tau(\omega_l) P(\mathbf{x},\mathbf{y}_j;\omega_l)h_{ij}h_{in}(\omega_l)P(\mathbf{y}_n,\mathbf{x};\omega_l)\Big|^2
\end{aligned}
$$

Using the Gaussian rule for the fourth order moments we obtain

$$
\mathbb{E}|u(\mathbf{x})|^2 \approx \big|\mathbb{E}u(\mathbf{x})\big|^2 + O(\eta^2\mu^2 BMN^3 + \eta^4 BMN^2).
$$

# Stability Condition

Then the stability condition

$$\Re(\mathbf{x}) = \frac{O(\mu^4 B^2 N^4)}{O(\eta^2 \mu^2 BMN^3 + \eta^4 BMN^2)} \rightarrow \infty$$

Therefore, for an active array and in the regime that $KN$ is bounded away from zero we have $\Re \rightarrow \infty$ when $KBN \gg M$.

# Point Target

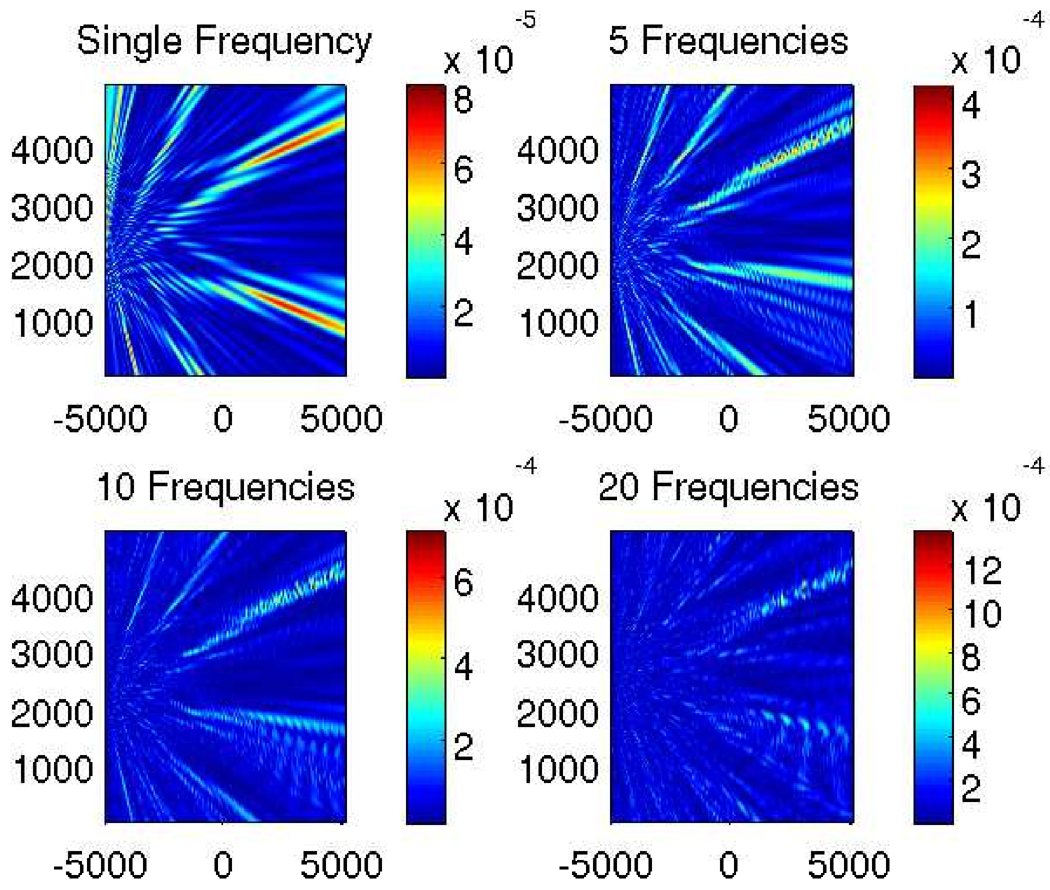


Fig $1$: Target is located at $(3000, 4000)$ and wavelengths are $52, 54, \ldots, 90$.

# Point Target (Zoom in)

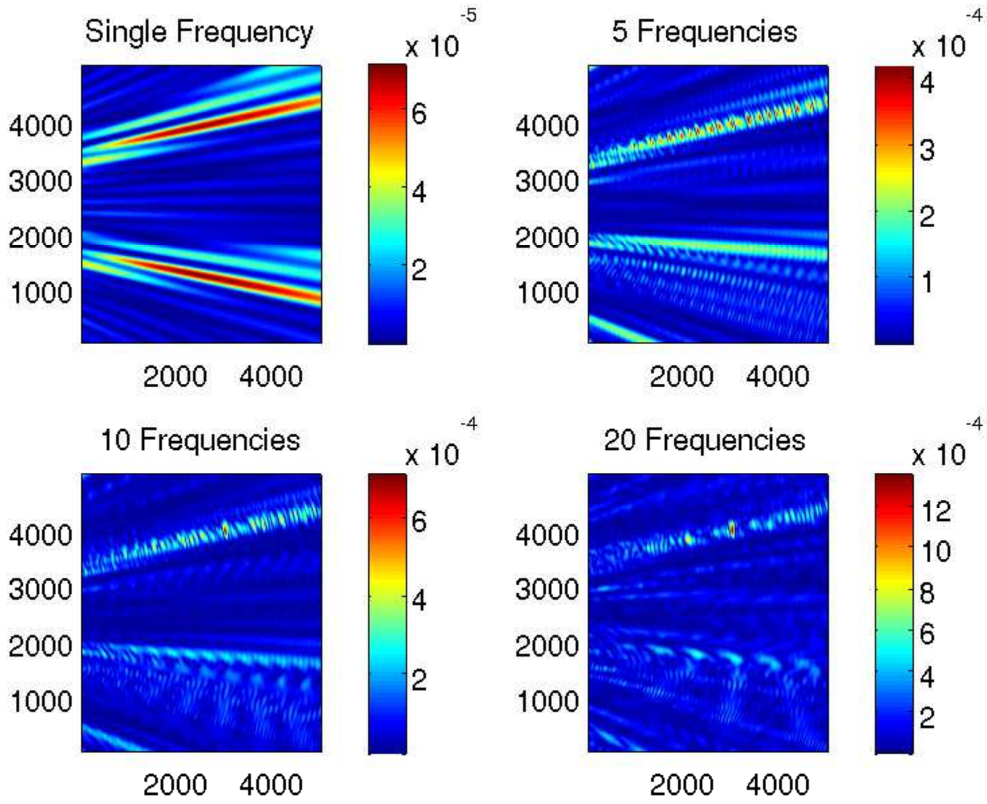

# Multiple Targets

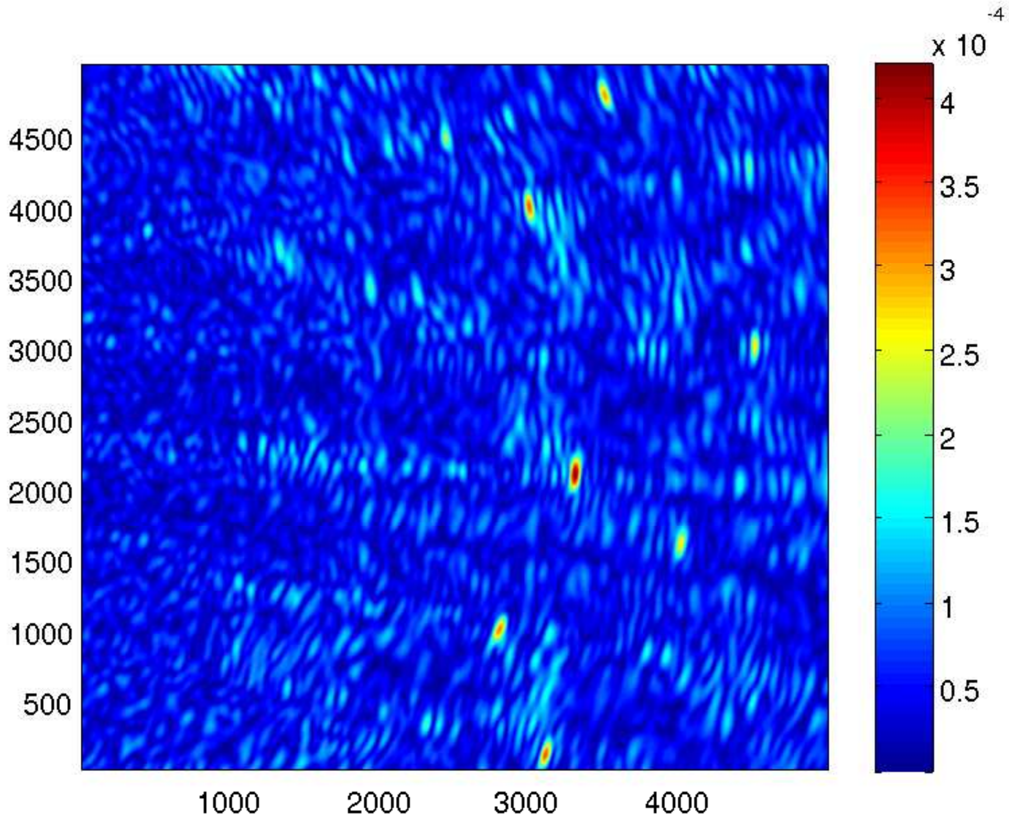


Fig 2: We fix the aperture size $2000$ and use only $6$ transducers to image $7$ targets.

sd

# Multiple Targets (SAR)

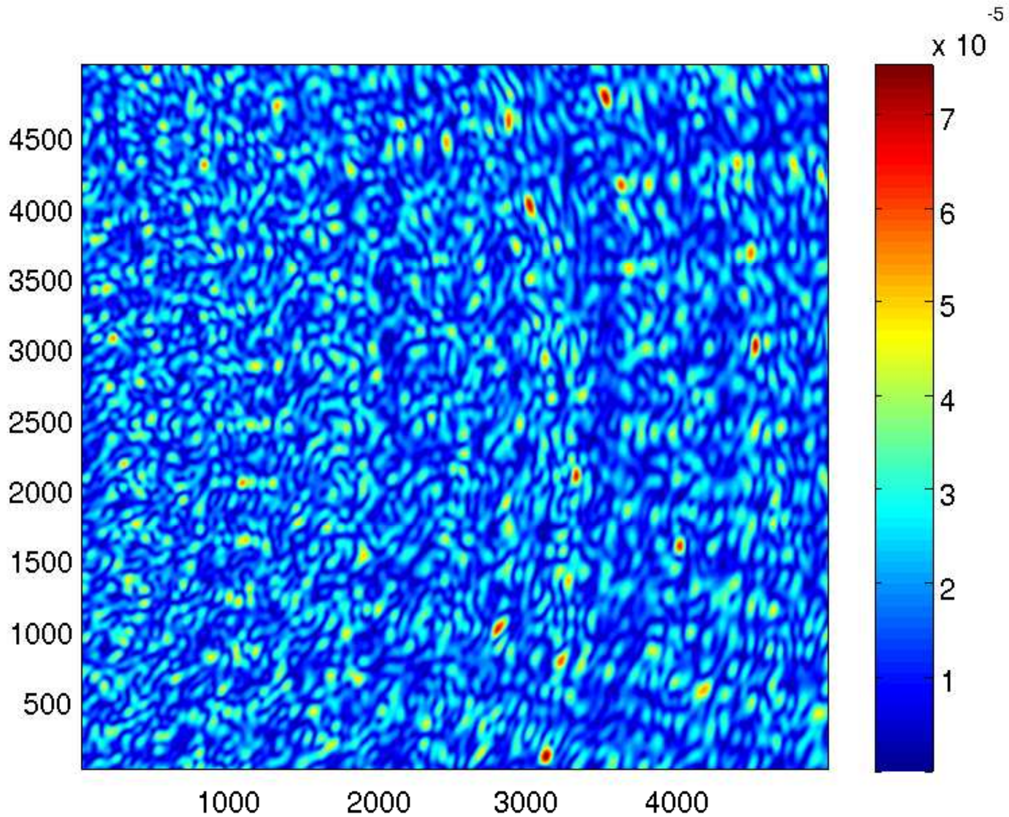


Fig $3$: We fix the aperture size $2000$ and use only $6$ transducers to image $7$ targets in the synthetic aperture case. Question: Can we improve the stability?

sd

# Statistical Detection

We can use the statistical method to find the locations of the targets.
In the imaging function, we drop the second order perturbation terms of $h$, which yields

$$
\begin{aligned}
u(\mathbf{x}) &= \mathbb{R}\Big\{ \sum_{l=1}^{B} \sum_{i=1}^{M} \sum_{j,n=1}^{N} \tau_i(\omega_l) P(\mathbf{x}, \mathbf{y}_j; \omega_l) \big( \bar{H}_{ij}(\omega_l) \bar{H}_{in}(\omega_l) \\
&\quad + \bar{H}_{ij}(\omega_l) h_{in}(\omega_l) + h_{ij}(\omega_l) \bar{H}_{in}(\omega_l) \big) P(\mathbf{y}_n, \mathbf{x}; \omega_l) \Big\}.
\end{aligned}
$$

At any imaging location $\mathbf{x}$, we set up two hypotheses:

$$
\begin{cases}
\mathcal{H}_0(\mathbf{x}): & \mathbf{x} \notin \{\mathbf{x}_1, \mathbf{x}_2, \ldots, \mathbf{x}_M\} \\
\mathcal{H}_1(\mathbf{x}): & \mathbf{x} \in \{\mathbf{x}_1, \mathbf{x}_2, \ldots, \mathbf{x}_M\}
\end{cases}
$$

# Neyman-Pearson Lemma

When we take a hypothesis test between {$H_0$: No object} and {$H_1$: Object intrusion}, the ratio test that rejects $H_0$ in favor of $H_1$, is the most powerful test with a given false alarm rate.

$$
\begin{aligned}
& \frac{\text{p.d.f. of } u(\mathbf{x})|\mathcal{H}_1}{\text{p.d.f. of } u(\mathbf{x})|\mathcal{H}_0} \\
= \quad & \frac{1}{\sqrt{2\pi\sigma^2}} e^{-\frac{1}{2\sigma^2}(u-\lambda)^2} / \left( \frac{1}{\sqrt{2\pi\sigma^2}} e^{-\frac{1}{2\sigma^2}u^2} \right) \\
= \quad & e^{-\frac{1}{2\sigma^2}(-2u\lambda+\lambda^2)} > e^{\gamma}.
\end{aligned}
$$

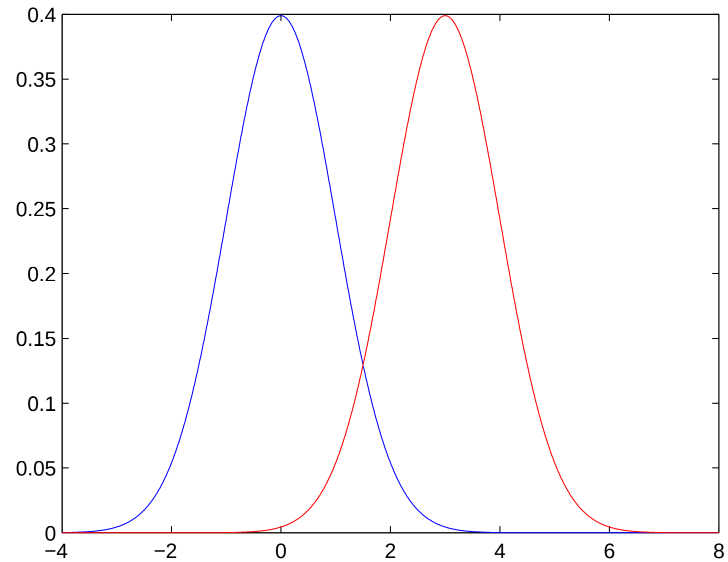

# Statistical Detection

$$\mathbb{E}(u(\mathbf{x})) = \mathbb{R}\{\sum_{l=1}^{B}\sum_{i=1}^{M}\sum_{j,n=1}^{N}\tau_i(\omega_l)P(\mathbf{x},\mathbf{y}_j;\omega_l)\bar{H}_{ij}(\omega_l)\bar{H}_{in}(\omega_l)P(\mathbf{y}_n,\mathbf{x};\omega_l)\},$$

$$\text{Var}(u(\mathbf{x})) = 2\eta^2 N\sum_{l=1}^{B}\sum_{i=1}^{M}|\tau_i(\omega_l)|^2||\sum_{j=1}^{N}\bar{H}_{ij}(\omega_l)||^2.$$

since $||P(\mathbf{x},\mathbf{y};\omega)|| = 1$. From the ratio test, we have

$$u > \frac{\gamma\sigma^2}{\lambda} + \frac{\lambda}{2}$$

# False Alarm Rate and Detection Rate

We denote $Q$ the left-tail probability function for a standard Gaussian random variable, $P_f$ the false-alarm rate, and $P_d$ the detection rate.

$$\begin{aligned}\mathcal{H}_0 &: \quad \frac{u(\mathbf{x})}{\sigma} = \frac{\gamma\sigma}{\lambda} + \frac{\lambda}{2\sigma} = Q^{-1}(1-P_f),\\ \mathcal{H}_1 &: \quad \frac{u(\mathbf{x})-\lambda}{\sigma} = \frac{\gamma\sigma}{\lambda} - \frac{\lambda}{2\sigma} = Q^{-1}(1-P_d).\end{aligned}$$

Then $P_f$ is related with $P_d$:

$$\begin{aligned}P_d &= 1 - Q(Q^{-1}(1-P_f) - \frac{\lambda}{\sigma})\\ \frac{\lambda}{\sigma} &= \sqrt{\frac{KBN}{2M}}.\end{aligned}$$

Conclusion: When $u > \sigma Q^{-1}(1-P_f)$, the detection says $\mathbf{x} \in \mathcal{H}_1$.

# ROC curve

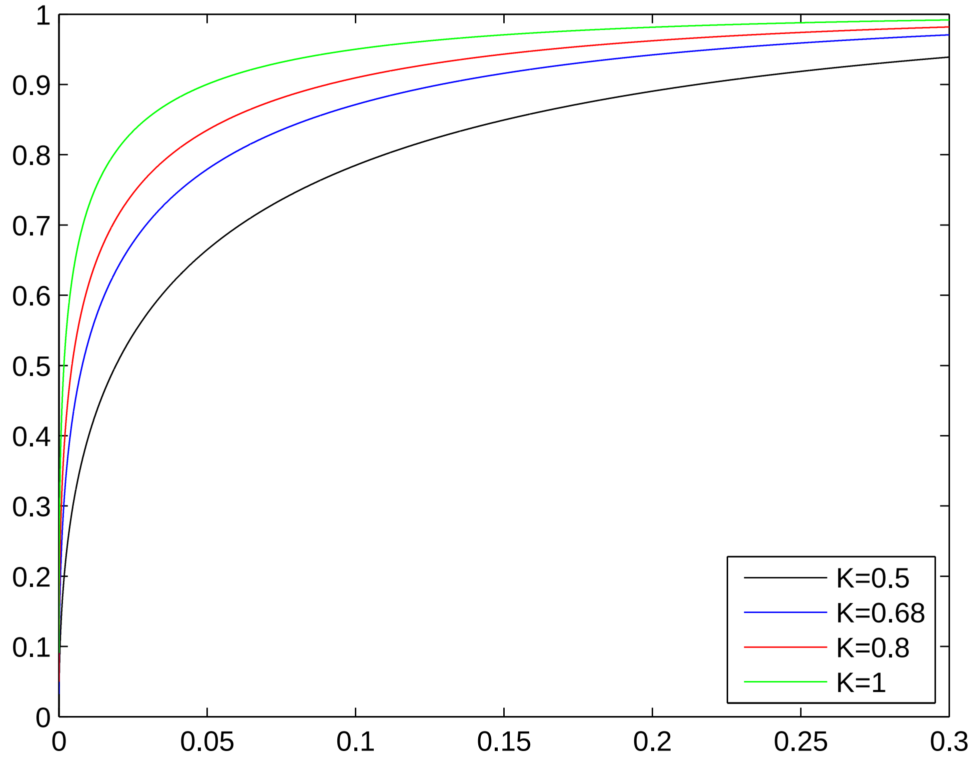


Fig $4$: The ROC curve is unique determined by $\sqrt{\frac{KBN}{2M}}$.

# Multiple Targets(Full responses)

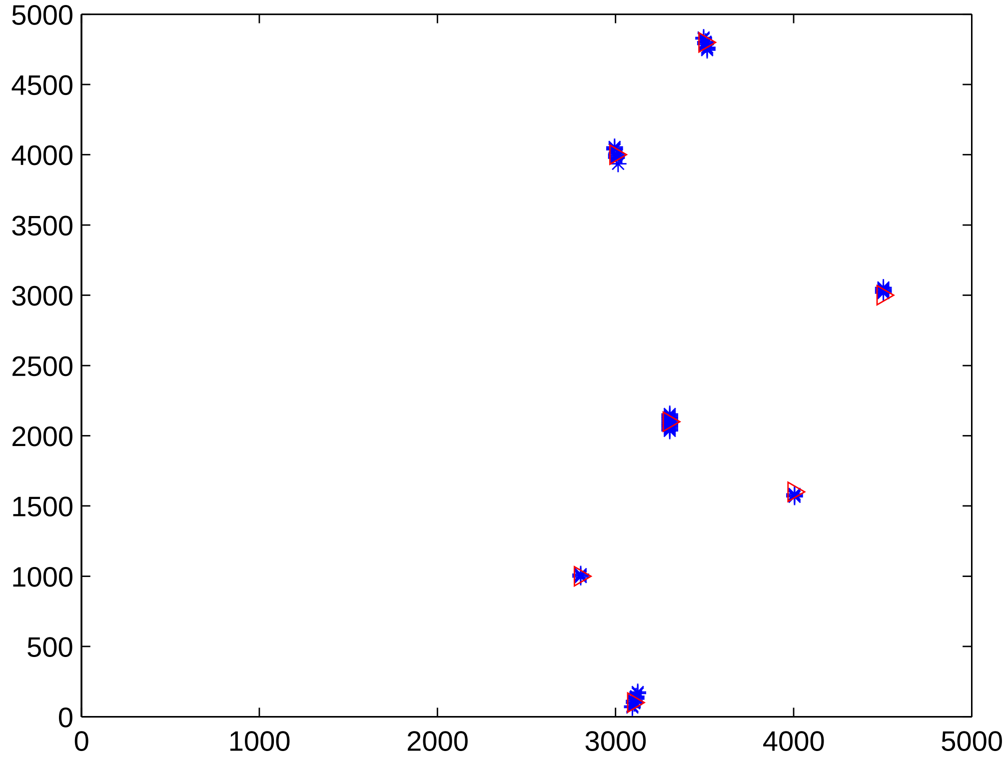


Fig $5$: We apply the statistical detection method to the imaging field we got in the previous multiple targets slide. The false-alarm-rate is $2.5\%$.

Original imaging plot

# Multiple Targets(SAR)

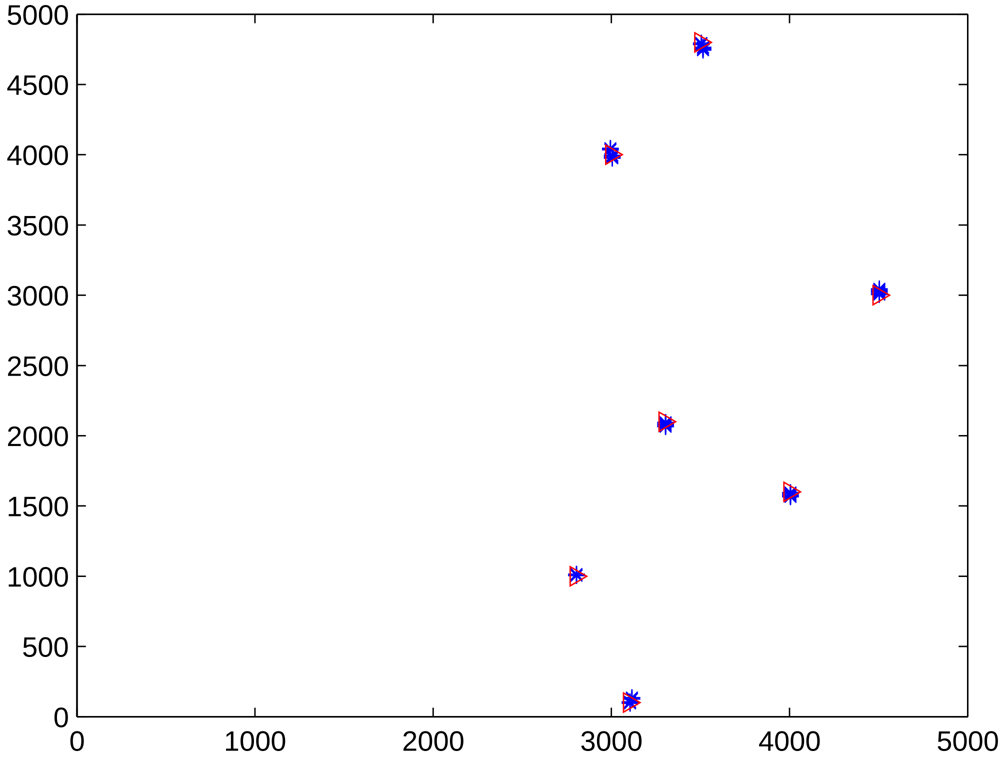


Fig 6: We apply the statistical detection method to the imaging field of multiple targets in SAR. The false-alarm-rate is $0.15\%$. The stability improved with the knowledge of the targets' number. Original imaging plot

# Outline

- Mathematical Models and Simulations
- Active Array Model and its Stability
- Passive Array Model and its Stability
- Conclusion

# Passive Array Model

The response vector with point source $\delta(\mathbf{x} - \mathbf{x}_i)$ is given by

$$\begin{pmatrix} H(\mathbf{x}_i, \mathbf{y}_1; \omega) \\ H(\mathbf{x}_i, \mathbf{y}_2; \omega) \\ \vdots \\ H(\mathbf{x}_i, \mathbf{y}_N; \omega) \end{pmatrix}$$

The imaging function is

$$\begin{aligned} u(\mathbf{x}) &= \sum_{l=1}^{B} \sum_{j=1}^{N} \sum_{i=1}^{M} \tau_i(\omega_l) P(\mathbf{x}, \mathbf{y}_j; \omega_l) H_{ij}(\omega_l) \\ &= \sum_{l=1}^{B} \sum_{j=1}^{N} \sum_{i=1}^{M} \tau_i(\omega_l) P(\mathbf{x}, \mathbf{y}_j; \omega_l) \left( \bar{H}_{ij}(\omega_l) + h_{ij}(\omega_l) \right) \end{aligned}$$

# Stability Condition

- Same stability condition:

$$\Re(\mathbf{x}) \equiv \frac{|\mathbb{E}u(\mathbf{x})|^2}{\mathbb{E}\big(|u|^2(\mathbf{x})\big) - |\mathbb{E}\big(u(\mathbf{x})\big)|^2} \to \infty$$

- Results: The imaging function is stable when $KBN \gg M$.
- The mean of the imaging function

$$\begin{aligned}
\mathbb{E}u(\mathbf{x}) &= \mathbb{E}\sum_{i=1}^{M}\sum_{l=1}^{B}\sum_{j=1}^{N}\tau(\omega_l)P(\mathbf{x},\mathbf{y}_j;\omega_l)\big(\bar{H}_{ij}(\omega_l)+h_{ij}(\omega_l)\big) \\
&= \sum_{i=1}^{M}\sum_{l=1}^{B}\sum_{j=1}^{N}\tau(\omega_l)P(\mathbf{x},\mathbf{y}_j;\omega_l)\bar{H}_{ij}(\omega_l) \\
&= O(\mu BN).
\end{aligned}$$

# Sketch of the Proof

$$
\begin{aligned}
\mathbb{E}|u(\mathbf{x})|^2 &= \mathbb{E}\Big\{ \sum_{l=1}^{B} \sum_{j=1}^{N} \sum_{i=1}^{M} \tau(\omega_l) P(\mathbf{x}, \mathbf{y}_j; \omega_l) \big(\bar{H}_{ij}(\omega_l) + h_{ij}(\omega_l)\big) \\
&\times \sum_{l'=1}^{B} \sum_{j'=1}^{N} \sum_{i'=1}^{M} \tau^*(\omega_{l'}) P^*(\mathbf{x}, \mathbf{y}_{j'}; \omega_{l'}) \big(\bar{H}^*_{i'j'}(\omega_{l'}) + h^*_{i'j'}(\omega_{l'})\big) \Big\} \\
&\approx \big|\mathbb{E}u(\mathbf{x})\big|^2 + \eta^2 M \sum_{l=1}^{B} \sum_{j=1}^{N} |\tau(\omega_l)|^2 \big|P(\mathbf{x}, \mathbf{y}_j; \omega_l)\big|^2 \\
&= \big|\mathbb{E}u(\mathbf{x})\big|^2 + O(\eta^2 BMN) \\
\Re &= \frac{O(\mu^2 B^2 N^2)}{O(\eta^2 BMN)} \to \infty
\end{aligned}
$$

It is clear that the imaging function is stable as $KBN \gg M$.

# Point Target

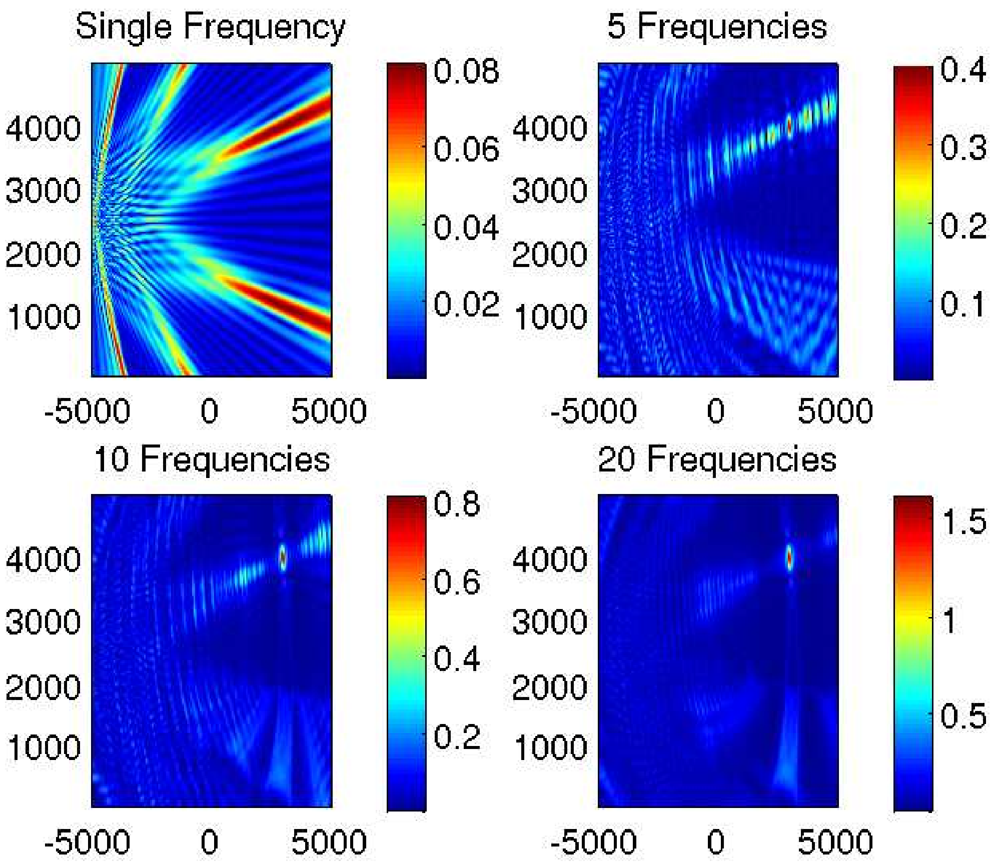


Fig 7: Target source is located at $(3000, 4000)$ and wavelengths are $52, 54, \ldots, 90$.

# Stability condition of the extended targets

The imaging function is

$$
\begin{aligned}
u(\mathbf{x}) &= \sum_{l=1}^{B}\sum_{j=1}^{N}\int_{x_i\in\Omega}\tau_i(\omega_l)P(\mathbf{x},\mathbf{y}_j;\omega_l)H(\mathbf{y}_j,\mathbf{x}_i;\omega_l) \\
\mathbb{E}u(\mathbf{x}) &= \sum_{l=1}^{B}\sum_{j=1}^{N}\int_{x_i\in\Omega}\tau_i(\omega_l)P(\mathbf{x},\mathbf{y}_j;\omega_l)\bar{H}(\mathbf{y}_j,\mathbf{x}_i;\omega_l) \\
&= O(BN(l_s)^d)
\end{aligned}
$$

where $l_s$ is the scattering mean-free path and satisfies

$$
|\bar{H}(\mathbf{x},\mathbf{y};\omega)| = e^{-\frac{r}{2l_s}}|G_0(\mathbf{x},\mathbf{y};\omega)|.
$$

# Stability Condition (Cont'd)

Assume the covariance function of the perturbation,

$$\mathbb{E}(h(\mathbf{x}_i, \mathbf{y}_j; \omega_l) h^*(\mathbf{x}_{i'}, \mathbf{y}_{j'}; \omega_{l'})) = \eta^2 F(\frac{\mathbf{x}_i - \mathbf{x}_{i'}}{l_c}) \delta_{jj'} \delta_{ll'}$$

where $l_c$ is the correlation length.

$$\begin{aligned}
\mathbb{E}|u(\mathbf{x})|^2 &= \mathbb{E} \sum_{l=1}^{B} \sum_{j=1}^{N} \int_{x_i \in \Omega} \tau_i(\omega_l) P(\mathbf{x}, \mathbf{y}_j; \omega_l) \big(\bar{H}_{ij}(\omega_l) + h_{ij}(\omega_l)\big) \\
&\times \sum_{l'=1}^{B} \sum_{j'=1}^{N} \int_{x_{i'} \in \Omega} \tau_{i'}^*(\omega_{l'}) P^*(\mathbf{x}, \mathbf{y}_{j'}; \omega_{l'}) \big(\bar{H}_{i'j'}^*(\omega_{l'}) + h_{i'j'}^*(\omega_{l'})\big) \\
&\approx |\mathbb{E}u(\mathbf{x}))|^2 + \eta^2 A(\Omega)(l_c)^d \sum_{l=1}^{B} \sum_{j=1}^{N} |\tau(\omega_l)|^2 |P(\mathbf{x}, \mathbf{y}_j; \omega_l)|^2 \int F(r) dr \\
&= |\mathbb{E}u(\mathbf{x}))|^2 + O(\eta^2 A(\Omega)(l_c)^d BN)
\end{aligned}$$

# Stability Condition

The stability condition of the extended target is

$$KBN \gg \frac{A(\Omega)(l_c)^d}{(l_s)^{2d}}$$

# Extended Targets

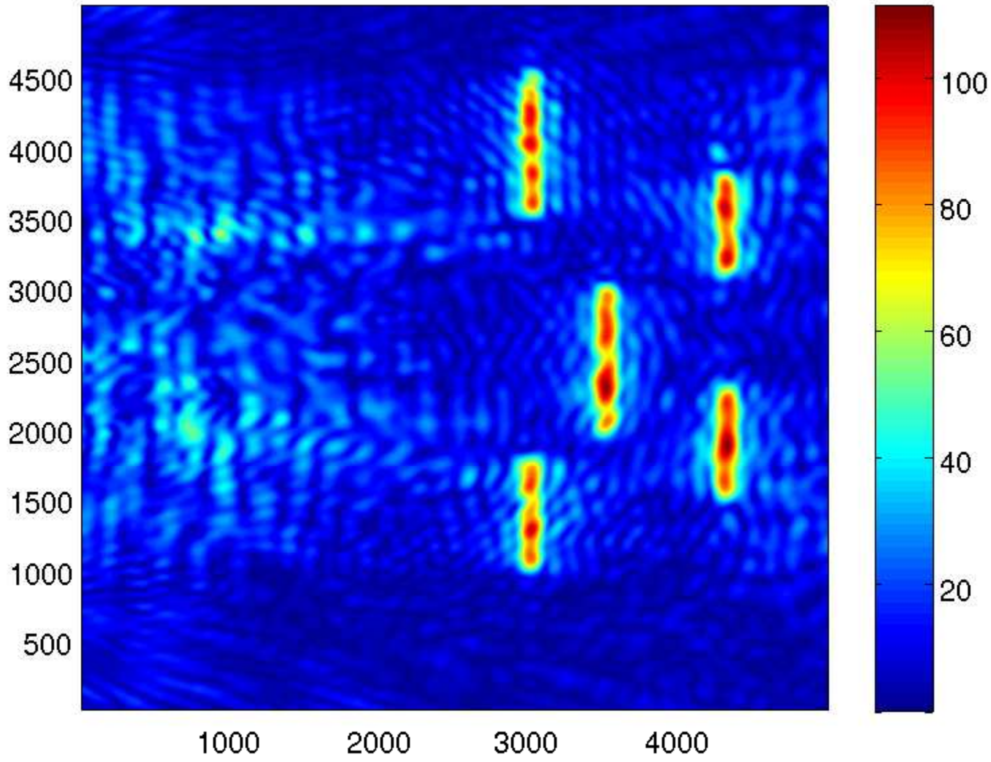


Fig $8$: Five lines of coherent sources are place in the media. The $51$ receivers are uniformly distributed at $x = -5000$ The reflectivity of the clutter is $70$.

# Mean and Free-space Green's function

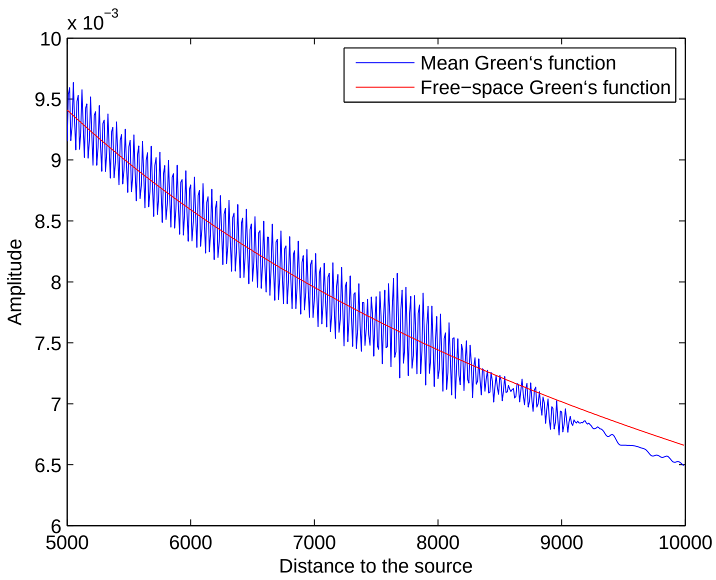


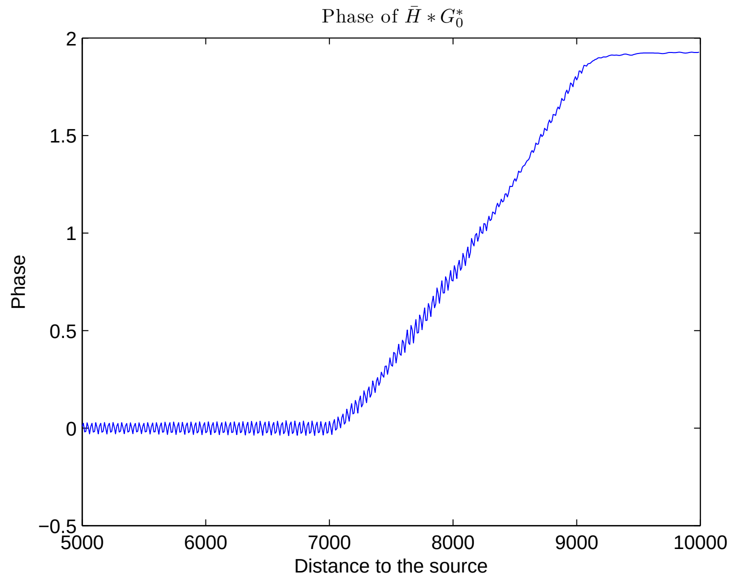


**(a) Amplitude Differences**

**(b) Phase of $\bar{H} * G_0^*$**

# Full and Free-space Green's function

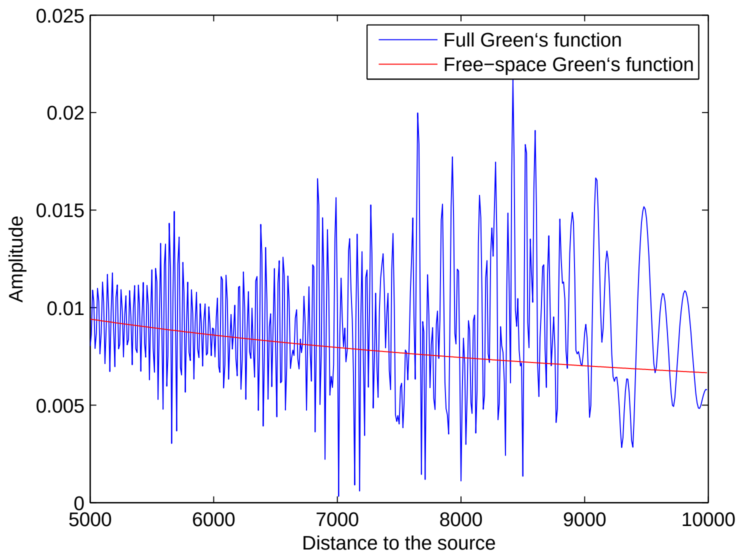


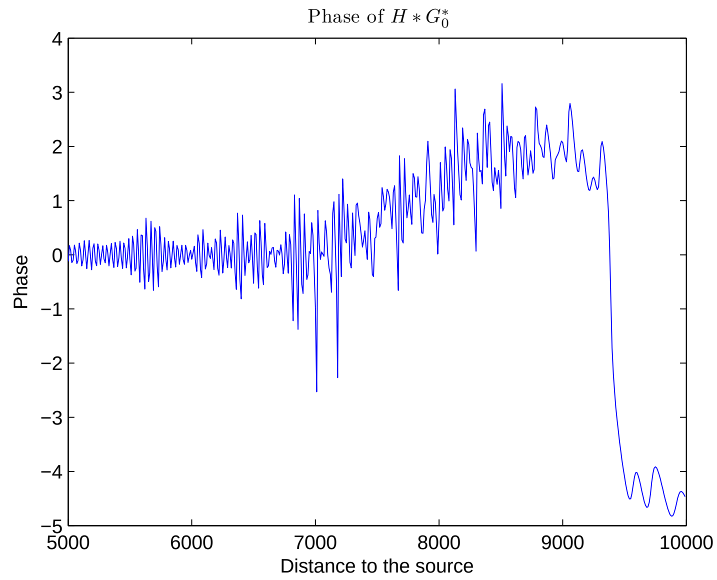


**(a) Amplitude Differences** **(b) Phase of $\bar{H} * G_0^*$**

# Conclusion

- Derived:
  - The stability conditions of the point targets: $KBN \gg M$. (Both in active and passive array models)
  - A statistical detection method – likelihood ratio test.
  - The stability condition of the extended targets: $KBN \gg A(\Omega)(l_c)^d/(l_s)^{2d}$.
- In the future:
  - Explore the mean Green's function.
  - Perturbed media in the Active Array Model.
  - Active array imaging of extended targets.